ELASTIC SCATTERING OF MEDIUM-ENERGY PROTONS

P. Schwandt, A. Nadasen, A.D. Bacher, M.D. Kaitchuck, J. Meek, P. Pile, P.P. Singh, and P.T. Debevec

Detailed angular distributions of elastically scattered protons have been measured for the set of targets, bombarding energies, angular ranges and angular intervals listed in Table 1.

Results for ^{208}Pb at 121.2 MeV and for ^{90}Zr at 79.8 and 135.1 MeV have been previously reported[1]. Examples of the results are illustrated in Figure 1 for ^{40}Ca and in Figure 2 for ^{208}Pb. When combined with the recent Maryland measurments[2] of similar extent and quality for ^{58}Ni, ^{90}Zr, ^{120}Sn and ^{208}Pb at 100 MeV, this new data set of 15 angular distributions adequately fills the void in high-quality proton elastic-scattering data which existed up to now in the energy region from 60 to 160 MeV. The present cross-section measurments will probably be extended to one additional energy close to 200 MeV

Table 1. Proton Elastic Scattering Measurements at IUCF

Target	E_p(MeV)	Θ_{Lab}	$\Delta\Theta$
^{28}Si	79.9	6-94°	2.5°
	135.1	6-86°	2.0°
^{40}Ca	80.2	6-93°	2.0°
	135.1	6-92°	2.0°
	160.0	6-90°	2.0°
^{90}Zr	79.8	6-90°	1.5°
	135.1	6-90°	1.5°
	160.0	6-81°	1.5°
^{208}Pb	79.9	6-93°	1.5°
	121.2	6-82°	1.0°
	180.0	6-77°	1.0°

once such beam is developed at IUCF within the next year and they will certainly be augmented later with polarization measurements after the IUCF polarized proton source has become operational in early 1978.

The measurements were carried out with isotopically-enriched targets (except for Si) of thickness from about 4 to 33 mg/cm^2. The scattered protons were detected using the QDDM spectrograph with a focal-plane array consisting of a helical wire chamber for position determination and 2 thin plastic scintillators for particle identification. Coincidence requirements defining the desired events resulted in very clean spectra, with backgrounds generally below one percent (except near 90° where the elastic cross section is of order 1 μb/sr). The overall energy resolution of 50 to 100 keV was more than adequate for this experiment. Angular resolution ranged from 0.3° to 1.5° with corresponding solid angles from 0.2 to 1.0

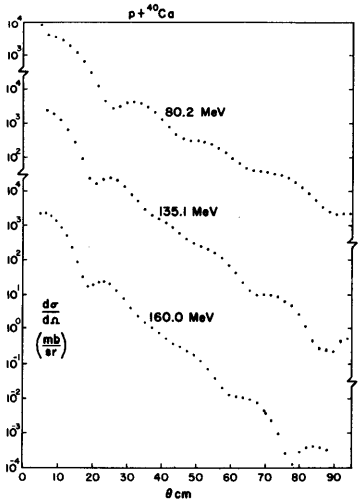

Figure 1.

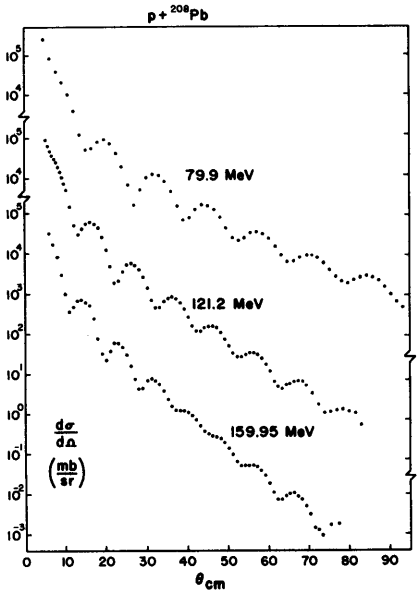

Figure 2.

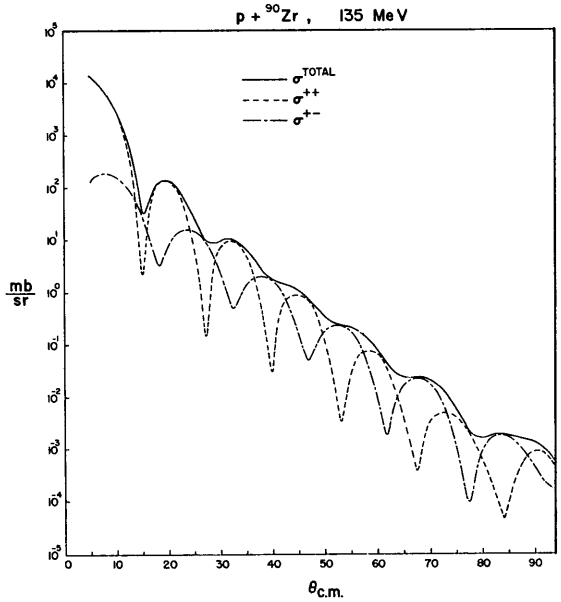

Figure 3.

msr. Beam intensities on target were held to 0.5-5nA with a water beam stop internal to the target chamber for the angular range 6° to ∿ 30°; for measurements from ∿ 30° to 90° (with the beam stopped in the shielded external beam dump) beam currents ranged from 15 to 150 nA. The overall relative accuracy of the data generally varies between ± 1% and ± 10%; the absolute cross sections are determined to within ± 10%.

The absolute elastic cross sections for most targets and energies span a range of values covering 6-8 orders of magnitude. One striking general feature of the data is the smoothing out of the diffraction structure in the mid-region of the angular range measured. This effect is most pronounced for the lighter targets (e.g. ^{40}Ca, Fig. 1) at all energies but is still seen even for ^{208}Pb at the highest energy (Fig. 2). Similar damping of diffraction patterns is also observed at somewhat lower energies for heavier projectiles (e.g. ^{4}He or ^{6}Li ions) where the effect arises from strong absorption and Coulomb effects. In the present case, for protons, the effect is found to be of entirely different origin: strong spin-orbit splitting of peripheral partial waves (i.e. with impact parameters in the surface region of the nucleus where the spin-orbit potential peaks) causes the spin-flip part of the cross-section to be sizeable forward of ∿ 90°. Both spin-flip and non-spin-flip parts, σ_{+-} and σ_{++}, (which add incoherently to produce the total observed cross section) oscillate strongly, as illustrated in Figure 3 for ^{90}Zr at 135 MeV. In the intermediate angular region they happen to have similar magnitude but opposite phase, while at far forward and back angles (> 100°) the non-spin-

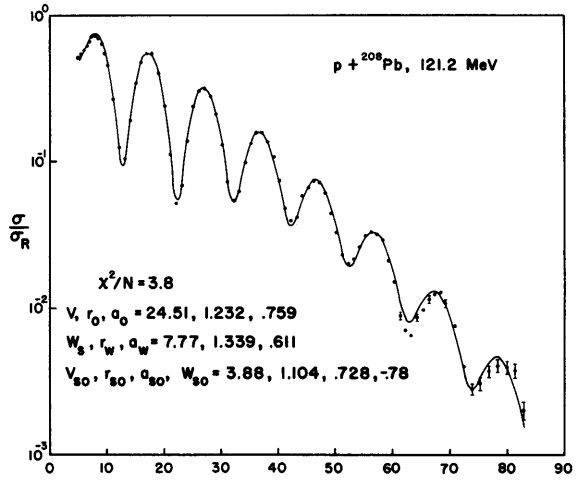

Figure 4.

flip part dominates. The rather large spin-orbit splitting seen at these high energies is a direct consequence of the sizeable spin-orbit potential strength for peripheral L-values (typically of order 10) relative to the appreciably weaker central potential, combined with the fact that a sizeable repulsive imaginary part to the spin-orbit interaction is required (resulting in strong j-dependence in the absorption). Relatively strong sensitivity of the differential cross section to spin-dependent interactions is thus encountered at these higher energies, in contrast to the fairly weak impact such interactions as a rule were found to have on this particular observable at lower energies.

One important motivation for the present measurements was to provide a more definitive optical-model parametrization of proton elastic scattering beyond 60 MeV than was previously possible with the small amount of available data of generally lower quality. In particular, the detailed nature of the energy variation of relevant characteristics of the local phenomenological potential (such as the volume integral per nucleon) is of considerable interest in relation to theoretical models of that energy dependence. To this end, optical-model fits to the present data were performed using the IUCF code SNOOPY6[3] with relativistic kinematics and a relativistic extension of the Schrödinger equation. A representative fit is shown in Figure 4 for ^{208}Pb at 121 MeV (parameter values given for the standard Woods-Saxon form factors are in MeV and fm). The volume integrals, J/A, of the real central potential obtained in these calculations for ^{208}Pb, for example, (Fig. 5) at 80, 100 and 121 MeV (the 160 MeV analysis is still in progress) are found to be

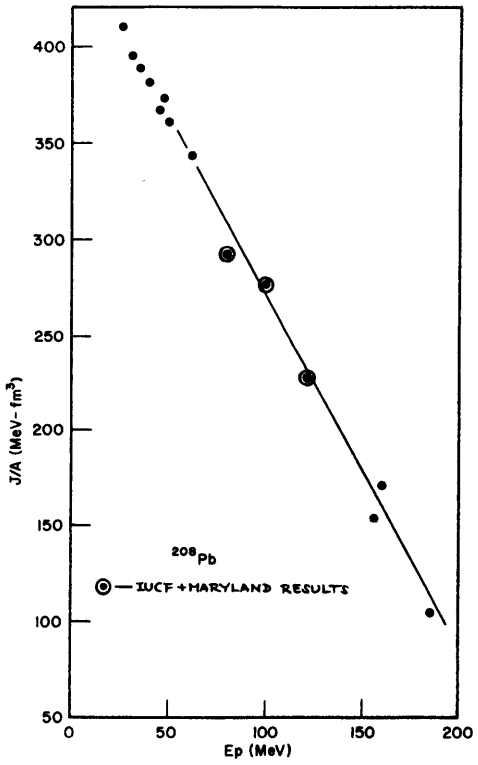

Figure 5.

consistent with earlier results[4] of similar relativistic calculations for lower and higher energies (non-relativistic calculations yield considerably larger values for J/A above 100 MeV).

Also currently underway are calculations of angular distributions in terms of microscopically-derived nucleon-nucleus potentials obtained in the Hartree-Fock approximation and using momentum and density-dependent effective interactions[5].

1) A. Nadasen et al., B.A. P.S. 21, 978 (1976).

2) K. Kwiatkowski, Ph.D. Thesis, University of Maryland (1976).

3) P. Schwandt, IUCF Intern. Report 76-2.

4) W.T.H. van Oers et al., Phys. Rev. C10, 307 (1974).

5) B. Sinha, Phys. Rev. C14, 404 (1976).